Transient Thermal Imaging Characterization of a Die Attached Optoelectronic Device on Silicon

Kazuaki Yazawa*[1,3], Dustin Kendig[1], Kadhair Al-hemyari[2], Ali Shakouri[3],
[1]Microsanj LLC,
[2]Intel Corporation,
[3]Birck Nanotechnology Center, Purdue University,

Microsanj LLC: 3287 Kifer Rd.,
Santa Clara, California, 95051, USA
Email: kaz@microsanj.com

ABSTRACT

Packaging of optoelectronic devices becomes more and more challenging due to higher heat generation per unit volume. We experimentally investigated the packaging thermal resistance for a semiconductor laser device and compared results for two material alternatives for the electrical passivation layer. We used the time-resolved thermoreflectance technique to obtain the time response for the thermal diffusion.

During this investigation, we also discovered another key factor related to the thermal resistance in addition to the passivation layer. The silicon substrate (~700 microns thick) also needs careful consideration for thermal diffusion. We observed some thermal islands across the thickness of the silicon substrate to diffuse and spread the heat. This local anisotropy, however, may be minor as the macroscopic temperature gradient is found to be reasonable. Nevertheless, this localized phenomenon may lead to performance variations in mass production. In the investigated package samples, minor voids and cracks were observed in the copper heat sink area. This may not be anticipated for final manufacturing, but these defects could result in localized higher thermal resistance for some of the arrayed device features on a chip.

By using the transient thermoreflectance technique, the heat diffusion process can be observed. This imaging technique enables us to track the temperature over a wide range of time. The time response curve provides an indication of the thermal heat sinking performance of the package structure. The transient thermal response clearly shows two stages of temperature rise. One is the spreading thermal diffusion in the silicon substrate and the other is thermal diffusion into the copper heat sink. The thermal mass for both, is within the time range. In this case, the opposite side of the device of the copper heat sink is connected to the thermal ground with a small thermal resistance.

The result demonstrates that a poly silicon passivation layer works better than silicon dioxide and decreases the thermal resistance by almost 30%.

KEY WORDS: time response, thermal imaging, passivation layer, thermal resistance, optoelectronics

NOMENCLATURE

C_{th}	thermoreflectance coefficient
R	reflective intensity, (J/m^2)
T	temperature, (K)
t	time, (s)

Greek symbols

α	thermal diffusivity, (m^2/s)
λ	wave length, (m)
μ	thermal diffusion length, (m)

INTRODUCTION

Optoelectronic devices, especially high performance semiconductor laser devices, dissipate a large amount of power per unit volume. This high power density requires very effective heat dissipation all the way to the heat sink. The packaging substrate, however, has to support power connections as well as provide good electrical insulation for two-terminal or multi-terminal devices. Following the Weidman-Franz law, the electrical conductivity and thermal conductivity for metals and semi-metallic materials are closely related. The electrical insulators also represent a large resistivity. Hence the fundamental conflict of electrical insulation and heat dissipation creates a significant challenge for the packaging of high heat flux optoelectronic devices.

For the purposes of thermal characterization, the device features, two dimensional offsets, and the complexity of a stacked structure are factors that complicate transient thermal measurement. A thermal response to a step input has been used to analyze a one dimensional structure including the thermal contacts to the substrate [1]. Normally, this method provides information based on an assumption of thermal resistance and capacitance. Possibly, even the asymmetric contact included in this system may not be an issue for comparison of cases where the fundamental structure does not change.

The thermal characterization of the device sometimes can be done by measuring the change in internal electrical resistance of the device. For a high power device, a device with inhomogeneous I-V characteristic, or a diode-like device, it is suitable to measure the temperature by an indirect contact method [2]. Since a linear assumption no longer applies, we utilized the time-resolved thermoreflectance imaging

technology to observe the thermal time response for the bar type semiconductor laser device mounted on a copper substrate to investigate the packaging thermal resistance for different electrical passivation layer materials.

TIME-RESOLVED THERMAL IMAGING

In this section, we describe the fundamentals of our non-invasive transient thermal imaging technique. The optical reflection from the surface of a solid is a function of temperature. The relationship between the change in reflectivity and the change in material temperature is usually expressed as a linear approximation when the temperature variation is small, e.g. 20 - 120 ^{o}C [3].

$$\frac{\Delta R}{R} = C_{th}(\lambda)\Delta T \qquad (1)$$

where, R is the intensity of the reflected light, T is the surface temperature, and C_{th} is the thermoreflectance coefficient, a constant that is wavelength and material dependent. The value of R depends on the imaging sensor, but as seen in Eq. (1) we take the relative change. Hence the absolute value of R does not affect the measurement of the temperature change relative to the reference temperature, i.e. usually room temperature. For most materials of interest the magnitude of the thermoreflectance coefficient, C_{th}, is relatively small, typically 10^{-2}/K to 10^{-5}/K, it is important therefore, to select an illumination wavelength that maximizes C_{th} so as to maximize the reflected signal to noise ratio (S/N). A detailed method for determining C_{th} is described in Ref. [4].

Transient thermal imaging is made possible by interlocking the signals driving the LED illumination, the device excitation, and the thermal imaging. The CCD imager has a shutter speed of only 30 frames per second, far slow to synchronize with the other signals, hence the shutter remains fully open during the CCD frame. The LED pulse is shifted a precise time after each excitation pulse is applied to provide a thermal image time series. In exchange for the capability of high time resolution, 100 ns for ordinal equipment [5] and a maximum of 800 ps for the dedicated high time resolution setup [6], the incoming energy to the imaging sensor is weak, thus a long averaging time is required for this method. The signal timing chart is shown in Fig. 1. Additional details for time-resolved thermoreflectance are provided in Ref. [7].

THERMAL DIFFUSION LENGTH/TIME

Thermal diffusion is the phenomenon that contributes to the thermal resistance of the structure and the heat capacitance. A specific time after the excitation pulse is applied, the heat travels through the structure from the heat source toward the heat sink. A thermal gradient is thus formed following the Fourier law. The distance the heat travels in a given time is derived as shown in Eq. (2).

$$\mu = 2\sqrt{\alpha t} \qquad (2)$$

where, μ is thermal diffusion length [m], α is the thermal diffusivity [m^2/s] of the material, and t is time [s]. From the thermal diffusion length, the time to reach a distance by thermal diffusion can be estimated by knowing the material properties. Table 1 shows the diffusivities we are using and the estimated diffusion times versus the thickness . It is interesting to note that the thermal diffusivity for bulk silicon is similar (~Δ20%) to that of copper. This is due to silicon's lower density. Silicon dioxide, on the other hand, has a value two orders of magnitude lower than bulk silicon.

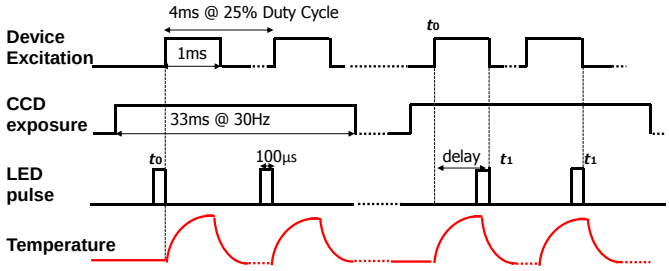

Fig. 1: Timing diagram for an example of transient thermoreflectance measurement.

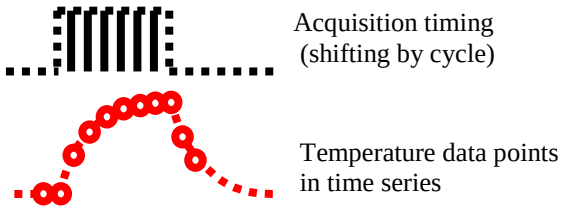

Fig. 2: Inter-locking transient imaging method: Temperature data points are acquired by shifting the timing delay each cycle to achieve a time resolution much smaller than the time scale of any of the system components , i.e. CCD: 33 ms, Bias: 1 ms, LED: 100 µs.

Table 1 Diffusion time by materials and thickness

Diffusion time estimations	SiO2	Si	Cu	Al	Ag	Au
Thermal diffusivity: α (m²/s)	8.30E-07	8.80E-05	1.11E-04	8.42E-05	1.55E-04	1.27E-04
thickness (µm)	diffusion time (µs)					
1	0.301	0.003	0.002	0.003	0.002	0.002
5	7.53	0.07	0.06	0.07	0.040	0.05
10	30.1	0.3	0.2	0.3	0.162	0.2
25	188	1.8	1.4	1.9	1.011	1.2
50	753	7.1	5.6	7.4	4.045	4.9
100	3,012	28.4	22.5	29.7	16.181	19.7
500	75,301	710.2	563.1	742.3	404.531	492.1
700	147,590	1,392.0	1,103.6	1,454.9	792.880	964.6

LASER DEVICE AND PACKAGE

The structure of the tested sample is shown in Fig. 3. DUT (device under test) in the figure represents the target laser device. The device is mounted on a 700 µm thick silicon substrate soldered (~170 µm thickness) to a copper base for the thermal heat dissipation. For electrical insulation, a passivation layer is in place between the device and the silicon

substrate. The material for the passivation layer was initially designed to be silicon dioxide and poly silicon considered as an alternate. Poly silicon has sufficient electrical insulation and has a higher thermal conductivity than SiO_2. As seen in Fig. 4, this device is constructed as a bar structure with an array of active regions.

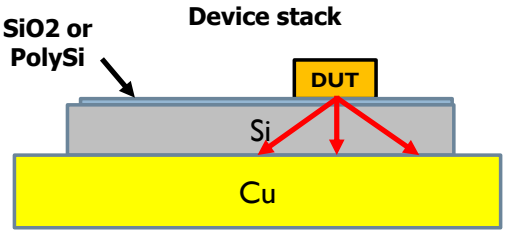

Fig. 3: Device vertical structure. DUT stands for device under test and the semiconductor laser device for this study. The passivation layer underneath the DUT is originally silicon dioxide and the poly silicon is considered as a replacement.

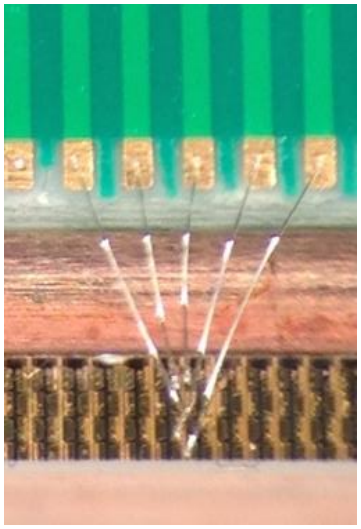

Fig. 4: Photo of the device in an array structure showing wire connections to other circuitry. The copper heat sink is in the middle and the device is the lower layer in this picture.

RESULT AND DISCUSSION

Temperature calibration was performed by applying a Type-K thermocouple directly on the device region with constant power applied. The temperature change in the copper right under the device is found to increase in temperature by 2.2 K at 420 mW.Fig. 5 shows the electrical characteristics of the device. The power dissipation appears to be consistent among the devices. Fig. 6 shows the temperature change versus applied power. The spread in this data is due to variations in the devices in an array. There are essentially three types of devices.

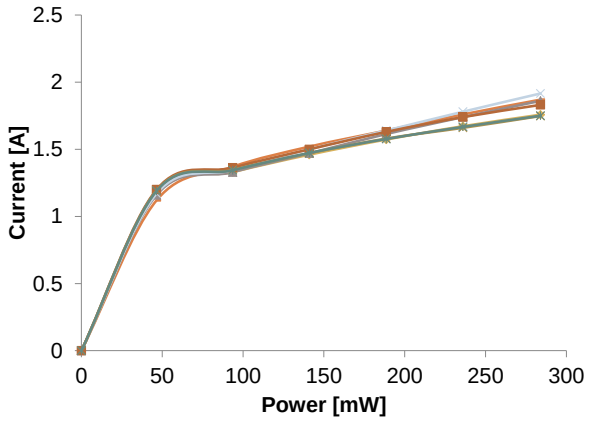

Fig. 5: I-V characteristics of DUT.

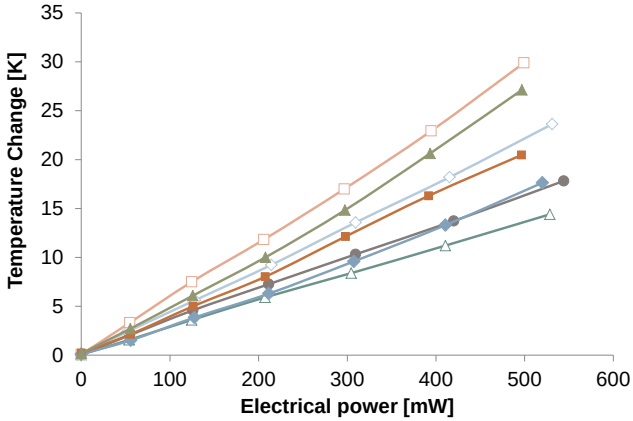

Fig. 6: Temperature correlation to the input electrical power in steady state.

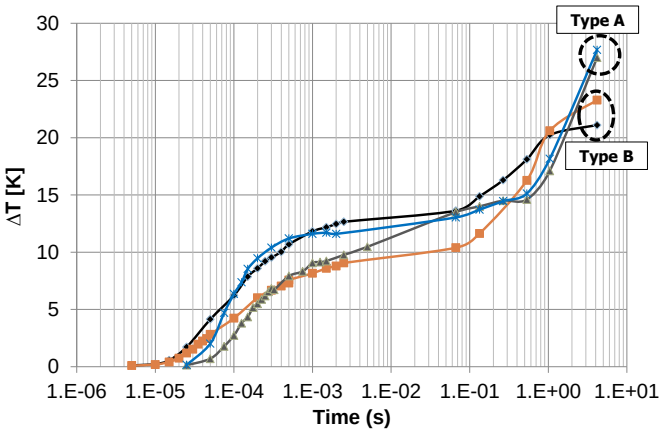

Fig. 7: Temperature time response for two types of devices.

Fig. 7 shows the temperature time response for two types of devices. There are two major time steps for the temperature change. The faster component time constant is about 1-1.5 ms and the latter one is in the range of seconds. The first time constant is due to the thermal diffusion through the silicon substrate, 1.4 ms for 700 mm thick substrate, and the other is due to the copper heat sink.

Fig. 8 shows the thermal profile image of the device array region with an optical image on the left and the thermal color contour on the right. The color bar shows the temperature

range of the image. Fig. 9 shows the profile of the temperature change along the line A-B in Fig. 8, depending on the time interval after the excitation pulse.

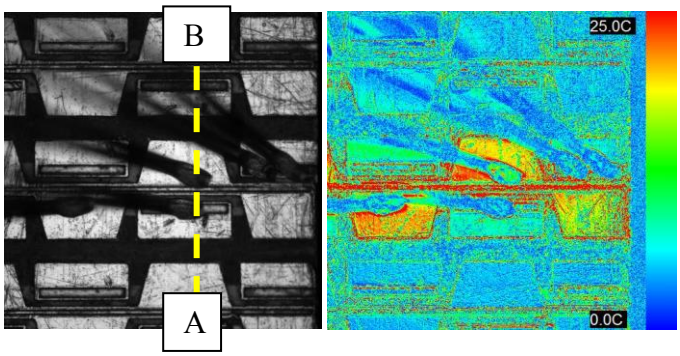

Fig. 8: Thermal image of the device array at 133 ms with 250 mA of current is applied. The temperature profile shown in the next figure is along the line A-B.

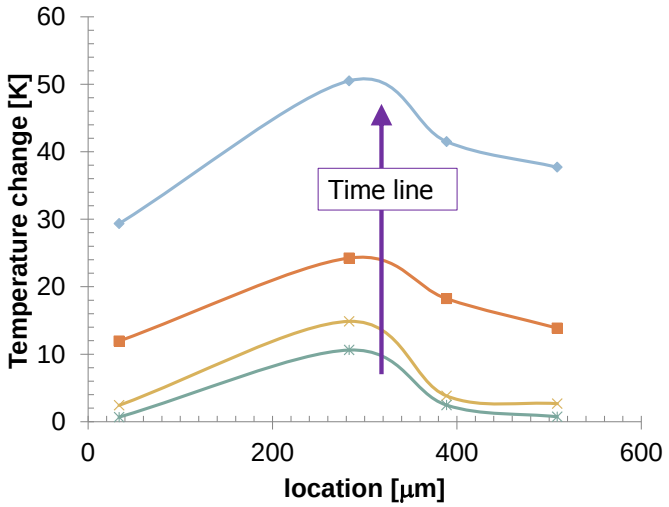

Fig. 9: Temperature profile along the line A-B in the array of device. The time after the pulse for the curves starts from the bottom $1.5x10^{-3}$ s, 0.133 s, 2 s, and 10 s to the top, respectively.

Fig. 10 shows the thermal profile across the silicon substrate thickness. The temperature is expressed by the color contour following the color scale shown at the bottom of the figure. This image is taken with a 5x microscope objective. A very thin red line on the top of the substrate represents the device. The large temperature gap between the device and the substrate is due to the thermal resistance of the passivation layer.

Table 2 summarizes the thermal resistance results with respect to time; 1 ms, 133 ms, and 10 s, and the change in thermal resistance due to changing the passivation layer from silicon dioxide to poly silicon. The improvement (reduction in thermal resistance) is observed to be almost 30%.

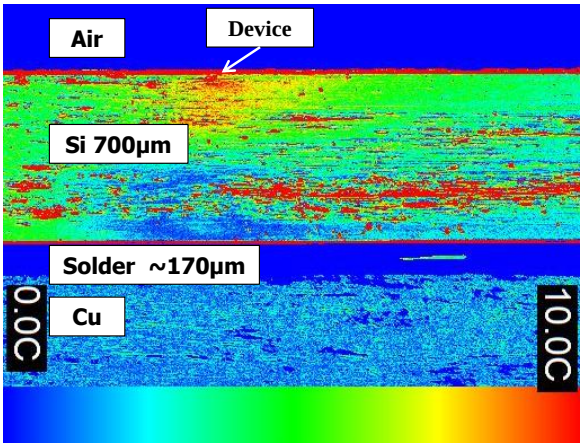

Fig. 10: Thermal profile across the substrate. The device is on the top. Applied current is 240 mA for 100 ms.

Table 2 Change in thermal resistance by changing passivation

Type	Thermal Resistance [K/W]				% Change			
	Optical	Thermorelfectance			Optical	Thermorelfectance		
		1.0 ms	133 ms	10 s		1.0 ms	133 ms	10 s
A	42.8		34.7	74.8	-20.9		-25.2	-34.9
B	43.6		26.8	51.8	-36.2		-23.6	
C		30.3	33.6	64.5		-27.3	-29.4	-25.4

Conclusions

By using the transient thermoreflectance technique, the heat diffusion process is observed in the laser optical device. The time response curve provides an indication of the thermal heat sinking capability of the package structure. The transient thermal response clearly shows two stages of temperature rise, where one is the spreading thermal diffusion in the silicon substrate and the other is the thermal diffusion into the copper heat sink through the solder joint. Both thermal masses are consistent with the time range. In this case, the opposite side of the copper heat sink is connected to the thermal ground with a small thermal resistance. Considering two alternatives for the passivation layer material, poly silicon works better than silicon dioxide and decreases the thermal resistance by almost 30%.

Acknowledgments

Authors thank to Dr. Christopher Cardenas (Intel Corporation) for helping us by providing the device samples and suggesting the thermal characteristics of the device for the measurements.

References

[1] Mentor Graphics, “Thermal Transient Tester Technical Information,”, http://www.mentor.com/products/mechanical/micred

[2] M. Farzaneh et al., “CCD-based thermoreflectance microscopy: principles and applications,” Journal of Physics D: Applied Physics 42, 143001, pp. 20, 2009.

[3] G. Tessier, et al., "Quantitative Thermoreflectance Imaging Calibration Method and Validation on a Dedicated Integrated Circuit," Proceedings of THERMINIC, 2005.
[4] K. Yazawa, et al., "Understanding the Thermoreflectance Coefficient for High Resolution Thermal Imaging of Microelectronic Devices," Technical Brief, Electronics Cooling Magazine, Issue March 2013, pp. 10-14, 2013.
[5] K. Yazawa, et al., "High Speed Transient Thermal imaging of Microelectronic Devices and Circuits," EDFA Magazine Volume 15, No 1, pp. 12-22, 2012.
[6] J. Christofferson, et al., "Picosecond Transient Thermal Imaging Using a CCD Based Thermoreflectance System," 14th International Heat Transfer Conference (IHTC14), 2010.
[7] K. Yazawa, et al., "Time-Resolved Thermoreflectance Imaging for Thermal Testing and Analysis," Proceedings of ISTFA 2013, 2013.